HHS Public Access

Author manuscript

Nat Struct Mol Biol. Author manuscript; available in PMC 2013 November 01.

Published in final edited form as:

Nat Struct Mol Biol. 2013 May ; 20(5): 611–619. doi:10.1038/nsmb.2549.

A conserved Mediator–CDK8 kinase module association regulates Mediator–RNA polymerase II interaction

Kuang-Lei Tsai[1], **Shigeo Sato**[2], **Chieri Tomomori-Sato**[2], **Ronald C. Conaway**[2,3], **Joan W. Conaway**[2,3], and **Francisco J. Asturias**[1]

[1]Department of Cell Biology, The Scripps Research Institute, La Jolla CA USA

[2]Stowers Institute for Medical Research, Kansas City MO USA

[3]Department of Biochemistry & Molecular Biology, Kansas University Medical Center, Kansas City KS USA

Abstract

The CDK8 kinase module (CKM) is a conserved, dissociable Mediator subcomplex whose component subunits were genetically linked to the RNA polymerase II (RNAPII) carboxy-terminal domain (CTD) and individually recognized as transcriptional repressors before Mediator was identified as a preeminent complex in eukaryotic transcription regulation. We used macromolecular electron microscopy and biochemistry to investigate the subunit organization, structure, and Mediator interaction of the *Saccharomyces cerevisiae* CKM. We found that interaction of the CKM with Mediator's Middle module interferes with CTD-dependent RNAPII binding to a previously unknown Middle module CTD-binding site targeted early on in a multi-step holoenzyme formation process. Taken together, our results reveal the basis for CKM repression, clarify the origin of the connection between CKM subunits and the CTD, and suggest that a combination of competitive interactions and conformational changes that facilitate holoenzyme formation underlie the Mediator mechanism.

INTRODUCTION

Transcriptional regulation is mainly focused on the initiation process, which entails recruitment of RNA polymerase II (RNAPII) and the general transcriptional factors to a promoter. Mediator, a multisubunit complex conserved throughout all eukaryotes, interacts with RNAPII and functions as a key regulator of RNAPII-dependent gene expression by integrating and conveying regulatory signals from activators and repressors to the basal transcription machinery[1–4]. The structure, subunit organization, and RNAPII interaction of Mediator are the subject of intense investigation because understanding them is essential for

Correspondence should be addressed to F.J.A. (asturias@scripps.edu).

AUTHOR CONTRIBUTIONS

All experiments, except those dealing with Mediator–CKM interaction in human cells, were designed by K-L. T. and F.A., and carried out by K-L. T. K-L. T. and F.A. discussed and interpreted results and wrote the manuscript. Human Mediator–CKM interaction experiments (Fig. 3) were designed, discussed, and interpreted by C.T.-S., S.S., R.C.C., and J.W.C. and carried out by C.T.-S. and S.S.

discerning the mechanism underlying transcription regulation. Mediator comprises 4 core structural modules[5] (Head, Middle, Tail, and Arm), plus a dissociable CDK8 kinase module (CKM), whose component subunits were individually recognized as transcriptional repressors[6] and genetically linked to the RNA polymerase II (RNAPII) carboxy-terminal domain (CTD)[7,8]. Recent studies suggest a more nuanced role for the CKM in both repression and activation[9] and mutations of CKM subunits have been associated with development of several malignancies[9–11].

In the yeast *Saccharomyces cerevisiae*, the CKM is a ~430 kDa protein complex that can reversibly associate with Mediator and includes 4 subunits[12,13]: Cdk8 (Srb10), CycC (Srb11), Med12 (Srb8), and Med13 (Srb9). CKM subunits were first identified through a genetic screen for mutations that would compensate for truncation of the CTD of Rpb1, the largest RNAPII subunit[7,8], which is essential for interaction of RNAPII with Mediator and a number of other complexes important in transcription and its regulation. In *in vitro* reconstituted transcription assays, Mediator lacking the CKM has a stimulatory effect on basal transcription[14,15]. In contrast, Mediator containing the CKM represses basal transcription[16,17], and genetic analysis indicates that the CKM is also involved in negative gene regulation *in vivo*[17]. It was initially suggested that the CKM would suppress transcription by phosphorylating the RNAPII CTD, but it was later discovered that CKM transcription repression is independent of its Cdk8 kinase activity[18,19]. On the other hand, it was reported that binding of the human CKM to Mediator interferes with RNAPII recruitment and represses transcription reinitiation[18].

Repression by the CKM in the absence of kinase activity could be related to the observation that the CKM has a direct effect on interaction of RNAPII with Mediator. Formation of a Mediator–RNAPII holoenzyme is largely blocked by association of the CKM with Mediator[19,20]. In *S. pombe*, it was proposed that the CKM prevents RNAPII interaction with Mediator by directly blocking the RNAPII binding site[19]. In contrast, studies in the human system led to the suggestion that the CKM inhibits polymerase interaction through an effect on Mediator conformation[18]. Interestingly, neither of these hypotheses explains why CKM subunits were identified in a genetic screen for CTD truncations.

We used a combination of macromolecular EM and biochemistry to study the interaction between Mediator and the CKM and investigate the mechanism behind the effect of the CKM on transcription initiation. We determined the structure and subunit organization of the *S. cerevisiae* CKM and characterized its interaction with core Mediator. We found that the structure, subunit organization, and mode of Mediator–CKM interaction, are conserved between yeast and humans. In yeast, the strongest Mediator–CKM interaction involved a discrete contact through subunit Med13 and biochemical and EM data indicated additional weaker interactions between the CKM and the Middle module. We discovered that Mediator–CKM interaction interferes with CTD-dependent RNAPII binding to a previously unknown site on the Middle Mediator module and with holoenzyme formation. In combination with biochemical results, our EM observations suggest that obstruction of CTD-dependent RNAPII interaction with the Middle module explains the repressive effect of the CKM on transcription and the observed genetic interaction between CKM subunit mutations and truncation of the RNAPII CTD.

RESULTS

Yeast CKM purification and EM structure

We purified native CKM from yeast using a tandem affinity purification (TAP) protocol[21]. SDS-PAGE analysis showed that tagging of CKM subunit Cdk8 resulted in purification of a complete, kinase-active CKM (Supplementary Note and Supplementary Fig. 1).

To investigate the CKM structure we imaged purified CKM particles in the electron microscope after preserving them in stain. EM images showed elongated particles that were well preserved and homogeneous in size and overall appearance (Fig. 1a). Two-dimensional (2D) class averages obtained after alignment and averaging of the images showed that the CKM is roughly 200 × 100 Å in size, with two bent features protruding from a globular central density (Fig. 1a, inset). The purity and conformational homogeneity of the purified CKM fractions allowed us to use the Random Conical Tilt technique[22] to determine an initial three-dimensional (3D) structure of the CKM (Fig. 1b) by using images of tilted and untilted CKM specimens. A more faithful view of the CKM structure came from a cryo-EM map of the complex at ~15 Å resolution calculated from ~70,000 CKM cryo-images (Fig. 1c, Supplementary Note and Supplementary Fig. 2).

Yeast CKM subunit organization

To understand the molecular organization of the yeast CKM, we set out to determine the position of individual subunits within the complex. The location of all four CKM component subunits was mapped through a combination of subunit deletion mutant imaging and antibody labeling. A calmodulin-binding peptide (CBP) left at the C-terminus of either Cdk8 or CycC after CKM purification from TAP-tagged strains could be localized by mixing the tagged, purified CKM with anti-CBP antibodies, followed by EM imaging after particle preservation in stain. After anti-CBP antibody labeling, 2D class averages calculated from Cdk8-TAP particles clearly showed antibody-like density around the distal portion of the bottom end of the CKM structure (Fig. 1d), pointing out the location of the Cdk8 subunit. Anti-CBP labeling of CycC showed that this subunit is adjacent to Cdk8, consistent with expected component interaction in this kinase-cyclin pair (Fig. 1e). To further confirm the position of Cdk8 within the CKM complex we purified CKM from a ΔCdk8 deletion strain and analyzed it by EM. Comparing a 2D class average calculated from wild-type CKM particles (Fig. 1f, top) with one obtained from ΔCdk8 CKM particles highlights the absence of a small piece of density at the same distal lower end of the CKM structure targeted by anti-CBP antibodies in the Cdk8-TAP particles (Fig. 1f, **middle**).

We were unable to TAP-tag the Med13 C-terminus for antibody labeling, but could localize Med13 through EM analysis of a ΔMed13 deletion strain generated in a CycC TAP-tag background (as with CycC, Med13 is non-essential and Med13 deletion results only in a phenotype of flocculation under standard culture conditions). A 2D class average from ΔMed13 CKM particles showed a structure much smaller than the wild-type complex. A difference map between the wild-type and ΔMed13 CKM 2D averages indicated that Med13 forms the top end of the CKM structure (Fig. 1f, *bottom*). Taken together with the results from Cdk8 and CycC localization, this implies that Med13 and the Cdk8-CycC kinase-

cyclin pair are at opposite ends of the CKM structure, connected by a central Med12 (Fig. 1g). Finally, the crystal structure of the human Cdk8-CycC complex[23] could be unambiguously fitted in a unique position and orientation into our cryo-EM reconstruction of the CKM complex, confirming our localization results for the Cdk8-CycC kinase-cyclin pair (Fig. 1h), and indicating that Cdk8 does not interact directly with either Med12 or Med13, but instead interfaces with Med12 through CycC.

Interaction of the CKM with Mediator

The human CKM has been reported to interact with Mediator through a contact involving CKM subunit Med13 and a "hook" at one end of the human Mediator structure[18]. We were interested in studying the Mediator–CKM interaction in yeast to shed light on the mechanism by which CKM impinges on Mediator regulation, and to investigate the origin of the genetic connection between the CKM and the CTD. We started by mixing purified yeast Mediator and CKM. Incubation of Mediator with CKM immobilized on a calmodulin resin through a CBP tag on the CycC C-terminus resulted in formation of a stable Mediator–CKM complex (Fig. 2a). Comparing averages obtained from images of Mediator–CKM complex particles to a 2D EM map of Mediator alone (Fig. 2b) indicated that, under the conditions of our binding experiment, Mediator and the CKM interacted in a number of ways. We observed a well-defined contact between one end of the CKM structure and the "hook" at the very end of the Mediator structure (Fig. 2c, middle, ~30% of particles), just as reported for the human CKM[18]. We also observed an additional, less frequent contact between the opposite end of the CKM structure and a point on the back side of the Middle Mediator module (Fig. 2c, right, ~10% of particles). In about 60 % of particles, the CKM had an extended interface with Mediator (Fig. 2c, left). In fact, careful clustering of Mediator–CKM particle images revealed a large repertoire of related interaction modes that can be better appreciated in an animation assembled by displaying different Mediator–CKM class averages in sequence (Supplementary Video 1).

Discrete, localized contacts between either end of the CKM and Mediator must involve subunits Med13 and Cdk8, which form the tips of the CKM structure. To unequivocally identify the CKM subunit interacting with the terminal Mediator hook, we repeated the Mediator–CKM interaction experiment using ΔCdk8 CKM and analyzed the resulting assemblies by EM. The resulting 2D class average (Fig. 2d) showed ΔCdk8 CKM bound to the hook, indicating that Med13 (at the end of the CKM structure opposite to Cdk8) is the subunit involved in interaction with the hook. Consequently, the CKM must contact the Mediator Middle module through subunit Cdk8. These conclusions are in agreement with a previous report about interaction of human Med13 with the hook at the end of the human Mediator structure[18], and with reported interaction of the Cdk8-CycC kinase-cyclin pair with subunits Med1 and Med4 in the yeast Middle Mediator module[24].

Two observations suggested that the contact between Med13 and the Mediator hook is the dominant interaction. First, EM analysis after incubation of ΔMed13 CKM with Mediator revealed only minimal complex formation, but EM analysis after incubation of ΔCdk8 CKM with Mediator showed formation of a complex in which the Med13 contact was established but the position of the ΔCdk8 CKM was highly variable (Fig. 2d). Second, in binding assays

in which immobilized ΔMed13 or ΔCdk8 CKM were incubated with Mediator, deletion of Med13 eliminated interaction of CKM with Mediator, whereas deletion of Cdk8 only weakened it (Fig. 2e). We were also able to determine maps that provided a 3D view of the predominant modes of yeast Mediator–CKM interaction (Figs. 2f–g and Supplementary Note).

The yeast CKM interacts with the Middle Mediator module

Interaction of the CKM with the top portion of the Mediator structure indicated that the Middle and Tail Mediator modules (module subunit composition listed in Supplementary Fig. 3a) could be involved in interaction with the CKM. We were able to purify a yeast Mediator subcomplex including all Middle module subunits from a ΔMed16 yeast Mediator strain (Supplementary Fig. 3b). Comparing 2D EM maps of Mediator and the Middle module indicated that Middle module subunits account for most, if not all of the Mediator density contacted by the CKM, including the hook at the end of the Mediator contacted by Med13 (Fig. 2h). Thus, although we cannot exclude the possibility of some contact between CKM and Tail module subunits, we conclude that the yeast CKM interacts primarily with Middle module subunits. This was confirmed by EM analysis following incubation of purified CKM and Middle module (not shown).

Conserved CKM organization and Mediator interaction

To directly compare the Mediator–CKM interaction in yeast and humans, we carried out EM and biochemical studies of the human Mediator–CKM interaction. First, we analyzed EM images of human Mediator–CKM particles[25]. A 2D map of free human Mediator showed a clear overall resemblance to a corresponding yeast Mediator map (Fig. 3a, *left*). In particular, the hook at the end of the human Mediator's Tail module appears remarkably similar to the corresponding portion of the yeast Mediator structure. We found that, as reported[18], the human CKM bound to the human Mediator's hook (Fig. 3a, **middle**, and Supplementary Fig. 3c–d). The overall structure of the human CKM appeared very similar to that of its yeast counterpart, which could be better appreciated if the human CKM was independently aligned to reduce blurring due to variability in its position with respect to human Mediator (Fig. 3a, *right*).

Next we turned to biochemical analysis to identify human CKM subunits involved in interaction with the human Mediator. We used siRNA to deplete specific CKM subunits in a HeLa cell line in which the MED19 subunit had been FLAG-tagged. FLAG-Med19-associated proteins were then immunopurified on anti-FLAG M2 agarose and analyzed by immunoblotting. MED12, MED13 (and the metazoan-specific MED13-like), remained associated with Mediator purified through the FLAG-MED19 tag after depletion of CDK8 or CycC (Fig. 3b, **left panel**). The entire CKM was displaced when both Med13 and Med13-like were depleted, but depletion of Med12 led to loss of Cdk8 and CycC without affecting association of Med13 or Med13-like with Mediator (Fig. 3b, **right panel**). These results coincide with our observations in the yeast system. Also, the human CKM subunit depletion results imply that the subunit organization of the human CKM mirrors that of the yeast CKM, with Med13 and Cdk8–CycC organized around a centrally-positioned Med12.

We then investigated which human Mediator subunits were involved in interaction with human CKM subunits Med13 and Med12. FLAG-tagged Med12 or Med13 were transiently transfected into HEK293T cells with individual c-Myc-tagged Mediator subunits. Tagged human CKM subunits were immunopurified on anti-FLAG M2 agarose resin, and co-purified cMyc-tagged Mediator subunits were analyzed by immunoblotting. Med13 interacted with human Middle module subunits Med1, Med26, Med19, and Med7 (Fig. 3c, *top*). Med12 also interacted with Med1 and Med26, but in addition it interactd with Med14, also a human Middle module subunit (Fig. 3c, *bottom*). Detection of a small amount of Med13 in cells not expressing FLAG-Med13 was due to the presence of a small amount of endogenous Med13. In addition, we could not determine if small amounts of Med7 and Med19 co-purified with Med12 because they interacted with it weakly, or if this was due to the presence of a small amount of endogenous Med13. We were not able to detect interactions between the CKM and individual human Tail module subunits (Fig. 3d). Therefore, human Mediator Middle module subunits are primarily responsible for interactions with Med13 (strong) and Med12 (weak) (Fig. 3e).

In conclusion, the Mediator–CKM interaction is largely conserved from yeast to humans and depends primarily on a strong contact between CKM subunit Med13 and Middle module subunits, with other CKM subunits (Med12 in humans; Cdk8 and CycC in yeast) establishing weaker interactions. To understand how these Mediator–CKM interactions might affect transcription regulation, we analyzed how the CKM affects the interaction of RNAPII and its CTD with Mediator.

CTD-binding to the Head and Middle Mediator modules

We examined the Mediator–CTD interaction by analyzing EM images recorded after incubation of Mediator and a full-length unphosphorylated CTD with a GST tag at the N-terminus (which could be directly visualized in EM images), or a full-length unphosphorylated CTD with a 6xHis-tag at the C-terminus (which could be localized through secondary labeling with an anti-His antibody). Consistent with previous reports of CTD binding to the yeast[26–28] and human[29] (Supplementary Fig. 4a) Head modules, EM images showed CTD density adjacent to the Head Mediator module (Fig. 4a). However, this accounted for only a small fraction (13% of particles) of observed CTD binding to Mediator and most CTD density (87% of particles) was observed at a previously unknown site in the Middle module (Fig. 4b). Close correspondence between the positions of the N-terminal GST tag and antibody density directed towards the C-terminal 6xHis tag on the CTD suggested that the unphosphorylated CTD adopts a compact conformation. Incubation of RNAPII purified through TAP-tagging of the CTD (which leaves a CBP-tag at the C-terminal end of the CTD) with anti-CBP antibodies indicated that the unphosphorylated CTD also adopts a compact conformation when attached to RNAPII (Supplementary Fig. 4b–c).

To confirm independent binding of the CTD to two different sites on Mediator, we incubated GST-CTD with purified Middle or recombinant Head modules and imaged the resulting complexes by EM. The resulting 2D class averages confirmed that the GST-CTD could bind to both the Head and Middle modules (Figs. 4c and d). The position of GST-

CTD on Head module was consistent with the position for CTD binding in the X-ray model of the Head-CTD complex[27]. Based on these results, we conclude that the CTD binds strongly to a previously unknown site on the Middle module and more weakly to a CTD-binding site on the Head module.

RNA polymerase II shows a variety of Mediator binding modes

To understand the connection between CTD and RNAPII binding to Mediator, we analyzed EM images recorded after incubation of purified Mediator and RNAPII. As expected[30], no RNAPII binding was observed if CTD-less RNAPII was incubated with Mediator. Incubation of wild-type RNAPII (alone or in combination with TFIIF) with Mediator resulted in a majority (~90%) of Mediator-RNAPII particles showing RNAPII at or near the CTD-binding site on the Middle module (Fig. 4e and Supplementary Video 2), and only a minority of particles showing RNAPII binding at its reported position near the Head module in the Mediator–RNAPII holoenzyme[31] (Supplementary Fig. 5a). This observation is consistent with predominant CTD binding to the Middle module.

To examine the possibility that binding of RNAPII to the Middle module might occur only when purified Mediator and RNAPII are incubated *in vitro*, we examined EM images of pre-formed Mediator–RNAPII "holoenzyme" particles purified directly from yeast by following the transcriptional activity of different fractions[31]. Analysis of these endogenous holoenzyme EM images with a stable clustering algorithm[32] revealed that RNAPII binds predominantly at two different places on Mediator. In about half the particles, RNAPII is found near the Head module and interacting with in a variety of ways (Fig. 4f). In the rest of the particles, RNAPII is located near the CTD binding site on the Middle Mediator module, as observed after incubation of Mediator with RNAPII *in vitro* (Fig. 4f). RNAPII binding near the Head module is consistent with published structures of the yeast[31] and human[20] holoenzymes, and with our recently published structure of a Head–minimal preinitiation complex assembly[33]. Variability in the precise mode of interaction between RNAPII and the Head could likely explain presumed differences in the precise orientation of RNAPII in the yeast and human holoenzymes.

Two observations suggest that holoenzyme formation might be a multi-step process initiated by CTD-dependent binding of RNAPII to the Middle module. First, analysis of the endogenous holoenzyme images also shows RNAPII bound to Mediator at positions spanning the distance between the Middle and Head module sites (Fig. 4f). Second, although RNAPII binds primarily to the Middle module after *in vitro* incubation of purified Mediator with RNAPII, the fraction of particles with RNAPII bound closer to the Head increases nearly 5-fold (from ~5% to >20%) if Mediator and RNAPII are incubated in the presence of a recombinant Gcn4 activator.

The CKM interferes with RNAPII binding to the Middle module

Overlap between the CKM and Middle module CTD-binding sites in yeast prompted us to investigate a possible effect of the CKM on Mediator–RNAPII interaction by incubating immobilized Med18 FLAG-tagged Mediator with RNAPII and wild-type, ΔMed13, or ΔCdk8 CKM. We found that RNAPII binding to Mediator decreased as the amount of wild-

type CKM increased (Fig. 5a, **lanes 4–6**). In contrast, ΔMed13 or ΔCdk8 CKMs, in which the Mediator–CKM interaction is compromised, were unable to diminish binding of RNAPII to Mediator (Fig. 5a, **lanes 7–9 and 10–12**, respectively). Biochemical studies first highlighted the importance of the CTD for polymerase interaction with Mediator[34] and EM observations showed that CTD-less RNAPII is unable to bind to Mediator[30]. Therefore, next we asked whether the effect of CKM on RNAPII binding to Mediator might directly involve the CTD. First, we performed binding assays to show interaction of the CTD with Mediator under our experimental conditions (Supplementary Fig. 5b). Next, we immobilized GST-CTD on beads and tested the effect of the CKM on interaction of the immobilized CTD with Mediator. We found that, as observed for RNAPII, binding of Mediator to the GST-CTD was diminished in the presence of wild-type CKM but not in the presence of ΔMed13 or ΔCdk8 CKM (Fig. 5b).

We also recorded EM images of yeast Mediator after incubation with both RNAPII and the CKM (Supplementary Fig. 6a–f). As expected considering the binding assay results, the CKM bound to Mediator, but RNAPII did not. This is explained by a large overlap between the binding positions for the CKM and RNAPII (Fig. 5c, Supplementary Videos 1 and 2, and Supplementary Fig. 6g). These results indicate that the effect of the CKM on the interaction between Mediator and RNAPII could be explained by CKM inhibition of CTD binding to the Middle Mediator module, which in turn could explain identification of CKM subunits in a genetic screen for mutations that compensate for CTD truncation[7,8].

Structure and Mediator interaction of CKM SRB mutants

We studied two SRB mutations, Srb8-1 and Srb10-1, involving CKM subunits Med12 and Cdk8, respectively, which compensate for CTD truncation[8]. The sequences of the Srb8-1 and Srb10-1 mutants had not been reported and we found that both mutations result in introduction of stop codons that prevent translation of the full *med12* and *cdk8* gene products. In the case of the *cdk8* Srb10-1 mutant, residue N473 is changed to a stop codon that prevents translation of the 83 C-terminal residues (corresponding to 15% of the protein length) of Cdk8. We purified CKM lacking the 83 C-terminal amino acids of Cdk8 by introducing the Srb10-1 mutation in a yeast strain in which CycC was TAP-tagged. SDS-PAGE analysis (Fig. 5d *left*) showed that deletion of the 83 Cdk8 C-terminal residues does not affect CKM integrity, and a 2D average of the Srb10-1 CKM mutant (Fig. 5d, *right*) was essentially identical to a wild type CKM class average (the mass of the missing 83 residues being too small to be easily detected in a low resolution 2D map). We also carried out CTD phosphorylation assays to test the effect of the Srb10-1 mutation on the CTD kinase activity of Cdk8 and found that the mutant's kinase activity is indistinguishable from wild-type (not shown). When we examined the interaction of the Srb10-1 CKM mutant with Mediator by EM, we found that binding of the mutant CKM to Mediator was diminished overall, and that the fraction of Mediator–CKM particles showing a contact involving the Cdk8–CycC end of the CKM was much lower than for wild-type CKM (Fig. 5e; ~10% and ~60%, respectively). Both of these observations are consistent with EM and biochemical data pointing to a contribution from the 83 C-terminal residues of Cdk8 to formation and stability of the Mediator–CKM complex.

As indicated above, the Srb8-1 Med12 mutation also resulted in introduction of a stop codon that replaced residue E375, preventing translation of 1053 (74% of total residues) C-terminal residues of Med12. Not surprisingly, this resulted in disruption of CKM integrity and only CycC and Cdk8 were recovered when we attempted purification of the mutant CKM from a strain bearing a TAP-tag at the CycC C-terminus (Fig. 5f). Based on our observations about Mediator–CKM interaction, we would definitely expect diminished interaction of the Srb8-1 mutant CKM with Mediator. Therefore, both the C-terminal truncation of Cdk8 in the Srb10-1 Cdk8 mutant, and disruption of CKM complex integrity in the Srb8-1 Med12 mutant, would result in diminished interaction of the CKM with Mediator. This suggests a possible common mechanism for compensation of CTD truncations by these SRB mutations: we hypothesize that a shortened CTD would partially hinder interaction of RNAPII with Mediator, and that such interaction is facilitated by reduction of steric hindrance to CTD binding from mutant CKM complexes showing decreased interaction with Mediator.

DISCUSSION

Our EM analysis of the yeast CKM revealed an elongated structure with the Cdk8-CycC kinase-cyclin pair and Med13 flanking a centrally positioned Med12 (Fig. 1g). There appears to be no direct interaction between Cdk8 and Med12, and Med13 does not seem to contact either Cdk8 or CycC. Yeast and human CKMs appear to be highly homologous, as evidenced by the similarity of their structures (Figs. 1, 3a), a close correspondence between the 3D structure of their Cdk8-CycC kinase pairs (Fig. 1h), and comparable interaction with Mediator through a strong interaction involving CKM subunit Med13 and a hook-like feature formed by Middle module subunits at one end of the Mediator structure (Figs. 2c and 3a and Supplementary Fig. 3c–d).

It has been reported that CKM transcription repression is independent of its Cdk8 kinase activity[18,19] (also see Supplementary Note). Our observations suggest that CKM repression is due to an effect on CTD binding to Mediator and holoenzyme formation (Fig. 6). We found that the CKM competes with RNAPII for interaction with Mediator (Fig. 5a and b), and that binding of the CKM to Mediator interferes with CTD-dependent RNAPII interaction with Mediator (Supplementary Fig. 6g). We show here that although incubation of yeast Mediator and RNAPII results in formation of some holoenzyme particles, a recombinant CTD or RNAPII are mostly seen binding to a site on the Middle module that overlaps with the CKM interaction site (Fig. 4). In addition, the proportion of holoenzyme particles is increased several fold if Mediator and RNAPII are incubated in the presence of an activator. We also show that Mediator–RNAPII particles isolated directly from yeast show RNAPII binding to Mediator in various positions covering the range from Middle- to Head-module binding. We believe that CTD-dependent binding of RNAPII to the backside of the Middle module likely represents an early step in the holoenzyme formation process that can be blocked by CKM binding (Fig. 6). The proposition that the CKM interferes with an early step in preinitiation complex formation is consistent with reports that the CKM has no effect on transcription by an already-formed PIC[6,18], and also with our observation that the presence of activator-facilitated formation of a full Mediator–RNAPII holoenzyme.

CKM interference with CTD-dependent Mediator–RNAPII interaction explains why components of the yeast CKM were first identified in a screen for mutations that compensate for truncation of the RNAPII CTD. If partial truncation of the CTD decreases CTD binding to Mediator, disruption of CKM's structural integrity, or abatement of its interaction with Mediator, would facilitate it. Consistent with this argument, two CKM mutations with a compensatory effect for CTD truncation, an Srb10-1 Cdk8 mutation that stops translation of the 83 C-terminal residues of Cdk8 and diminishes Mediator interaction without affecting kinase activity, and an Srb8-1 Med12 mutation that stops translation of 1053 C-terminal residues and results in disruption of CKM integrity, result in decreased interaction of the CKM with Mediator.

We have reported that interaction of RNAPII with the Head module results in a polymerase conformation change and a measurable increase in transcription[33]. Interaction of RNAPII with the Head module could represent the final stage in the holoenzyme formation process. Modulation of holoenzyme formation, for example through interference by the CKM with CTD–dependent RNAPII interaction with the Middle Mediator module, or the effect of an activator that would help the transition of RNAPII from the Middle to the Head modules (presumably through some effect on Mediator conformation) may be critical for the mechanism of Mediator regulation.

EM analysis of yeast Mediator reveals a remarkable conformational flexibility. Mediator is extremely pliable and we have not detected long-range correlations between the conformations of different portions of the Mediator structure[5]. This would seem to argue against a model for the Mediator mechanism in which a specific binding event (e.g., binding of the CKM or an activator) would result in a single well-defined Mediator conformation that could directly lead to a specific functional outcome (e.g., activation of transcription from a specific promoter). Conformational analysis of other macromolecular complexes, such as the ribosome[35] or mammalian fatty acid synthase[36], indicate that they can access a number of related conformations and that it is only the distribution of particles between these possible conformations that is altered by interaction with a given factor. We believe that the results from our study of the Mediator-CKM interaction illustrate the complexity of Mediator regulation, and suggest that competition amongst different factors for binding to Mediator could be a fundamental aspect of the Mediator regulation mechanism.

ONLINE METHODS

Yeast Strains

Yeast gene manipulations were carried out using standard protocols. The protease-deficient yeast strain BJ2168 (ATCC, 208277) was used for TAP-tagging of Mediator or the CKM for protein purification. A PCR-based genomic epitope-tagging method was used to construct yeast strains with different kinds of affinity epitopes. For TAP-tagging of CycC, Cdk8, Med7, Med22, or Rpb1, the pBS1479 plasmid was used to introduce a TAP-tag at the C-terminus of the targeted protein. For FLAG-tagging of Mediator, the pFA6a-FLAG-kanMX6 plasmid was used to introduce a 3xFLAG-tag at the C-terminus of Med18 in a strain in which Mediator subunit Med22 had bee TAP-tagged for purification. For subunit deletion or truncation, a PCR-amplified kanMX6 cassette from plasmid pFA6a-kanMX6

was used to replace either a specific region, or the entirety of an open reading frame. Yeast strains used in this study are listed in Supplementary Table 1.

Purification of CKM and Mediator

Yeast cells were grown in 2X YPD medium. Cells were harvested, washed, and resuspended using purification buffer (50 mM HEPES, pH 7.6, 300mM KOAc, 0.5 mM EDTA, 5 mM β-ME, 10% (v/v) glycerol, 0.1% (v/v) NP-40, and protease inhibitors). CKM isolation was carried out by following a standard TAP purification procedure as described[21]. For purification of wild-type CKM, TAP tags were inserted at the C-terminus of the Cdk8 or CycC subunits of the CKM. For purification of ΔMed13 CDK8, ΔCdk8 CKM, Srb10-1, and Srb8-1 CKM, the TAP tags were inserted at the C-terminus of the CycC subunit. Mediator was purified using the TAP method, combined with ammonium sulfate precipitation essentially as described[5]. Purified protein complexes were analyzed by SDS-PAGE and examined by EM.

Electron Microscopy and Image Processing

Stained specimens of CKM, Mediator–CKM, and Mediator–RNAPII were preserved with 2% (w/v) uranyl acetate as described[37]. Images were recorded at a magnification of 50,000X on a 4,096 × 4,096 CCD detector (Gatan, Inc.) with a Tecnai F20 electron microscope (FEI), operating at an acceleration voltage of 120 kV. Images were recorded using low dose procedures, at ~0.5 μm underfocus. Two-fold pixel binning of the original CCD images resulted in a final pixel size of 4.34 Å. Image processing was carried out using the SPIDER[38] and SPARX[39] software packages. An initial 3D map of the CKM was calculated using the Random Conical Tilt (RCT) method[22] from tilt-pair images of ~6,000 CDK8 particles. The same protocol was used to obtain RCT reconstructions of Mediator–CKM and Mediator–RNAPII using 2065 and 2540 tilt-pair images, respectively.

Cryo-EM samples of CKM were also prepared as described[37] and imaged under low-dosed conditions using the same microscope and settings, but recorded on SO-163 film (Kodak) at a magnification of 50,000X and at 1.5–4.0 μm underfocus values. Film images were digitized using a Nikon Super Coolscan scanner. Digitized images were two-fold pixel averaged to 2.54 Å per pixel. CKM particle images (~70,000) were selected using Dogpicker[40]. A cryo-EM map of the CKM was calculated by projection-matching refinement, using the RCT reconstruction the CKM as initial reference. Three-dimensional structure interpretation, docking of the Cdk8-CycC complex X-ray model[23], and image rendering, were carried out using UCSF-Chimera[41].

CKM-Mediator Interaction and Binding Assays

To form a Mediator-CKM complex, we incubated purified Mediator and CDK8 (3:1 molar ratio) and separated the complex by incubating it with a calmodulin bead resin (Stratagene) (the CKM had a CBP tag on Cdk8, but Mediator was purified using a modified TAP tag in which the CBP was replaced by 10xHis). For binding experiments, we immobilized ~300 ng of CBP–tagged wild-type, ΔMed13, or ΔCdk8 CKM on 10 μL of calmodulin bead resin, in binding buffer (20 mM HEPES, pH 7.6, 200mM KOAc, 10% (v/v) glycerol, 5 mM β-mercaptoethanol, 0.1% NP-40) containing 1 mM $CaCl_2$. We incubated the resin alone, or

with ~1 μg Mediator at 4°C for 2 h. After removal of the flow-through, we washed the resin three times with 400 μl binding buffer containing 1 mM $CaCl_2$. We eluted bound proteins by mixing the resin with 40 μL of binding buffer containing 5 mM EGTA, and analyzed the elution by SDS-PAGE and Western blotting.

Yeast Mediator-RNAPII-CKM Interaction Experiments

To assay Mediator-CKM-RNAPII interactions, we incubated purified wt, ΔMed13 or ΔCdk8 CKM with FLAG-tagged Mediator immobilized on 10 μl of ANTI-FLAG M2 Agarose resin (Sigma) in buffer A for 2h at 4°C. Then RNAPII was added and incubated for 2h at 4°C. Beads were washed three times, resuspended in 30 μL of 2 x SDS loading dye, and analyzed by SDS-PAGE and Western blotting. For Mediator-CKM-GST-CTD binding assays, purified Mediator was mixed with wt, ΔMed13 or ΔCdk8 CKM for 2h at 4°C and then incubated with 10 μL of GST-CTD-immobilized glutathione Sepharose beads (GE Health) in buffer (20 mM HEPES, pH 7.6, 250 mM KOAc, 10% glycerol, 0.1 % NP-40, protease inhibitors) for 2h at 4°C. Beads were washed with binding buffer three times, resuspended in 30 μl 2 x SDS loading dye, and analyzed by SDS-PAGE and Westernblotting.

Biochemical analysis of human Mediator–CKM interactions

Interactions between exogenously expressed human CKM subunits MED12 and MED13 and other Mediator subunits were performed essentially as described[42]. Briefly, HEK 293T cells were co-transfected with 4 μg each of pcDNA3.1 derivatives encoding FLAG-tagged MED12 or MED13 and cMyc-tagged Mediator subunits. 48 hours after transfection, whole cell lysates were prepared and subjected to anti-FLAG immunoprecipitation, and cell lysates and anti-FLAG immunoprecipitates were analyzed by western blotting using anti-FLAG M2 antibodies (Sigma, F3165) or anti-cMyc antibodies (Roche Applied Bioscience, 11667149001).

To define CKM subunits involved in the interaction with human Mediator, human HeLa S3 cells stably expressing FLAG-tagged MED19 were transfected with ON-TARGETplus SMARTpool siRNAs targeting human CycC (L-003209), CDK8 (L-003242), CDK19(L-004689), MED12(L-009092), MED13(L-019909), MED13-like(L-027126), MED15(L-017015), MED16(L-003736), MED23(L-013220), MED24(L-021247), MED25(L-014689), or ON-TARGETplus Non-targeting Pool (D-001810), all from Thermo Scientific. To generate HeLa cells expressing FLAG-MED19, cDNA encoding FLAG-MED19 was subcloned into pQCXIH (Clontech Laboratories, Inc.) and transfected into Plat-E 293T cells[43] to generate an ecotropic retrovirus. HeLa S3 cells stably expressing the retrovirus receptor mCAT were infected with FLAG-MED19 retrovirus, and hygromycin-resistant, FLAG-MED19-expressing clones were selected. To perform siRNA transfections, 2×10^6 FLAG-MED19 expressing cells were seeded onto 10 cm culture dishes and, after 24 hours, transfected with 30 nM of siRNA oligo using Lipofectamine RNAiMax (Life Technologies) according to the protocol recommended by Life Technologies. 72 hours after siRNA transfection, whole cell lysates were prepared and subjected to anti-FLAG immunoprecipitation, and cell lysates and anti-FLAG immunoprecipitates were analyzed by western blotting using antibodies against endogenous Mediator subunits. Anti-CycC (A301–989A), anti-MED12 (A300–774), anti-MED13 (A301–278A), and anti-MED1 (A300–

793A), were from Bethyl Laboratories, Inc.; anti-MED6 (sc-9433), anti-MED8 (sc-98482), and anti-MED26 (sc-81237) were from Santa Cruz Biotechnology, Inc.; anti-MED13-like (ab89831) and anti-MED31 (ab54761) were from AbCam; anti-MED21 H00009412-M05) was from Novus Biologicals; rabbit anti-MED25 serum was a generous gift from Michael Carey (UCLA); anti-peptide antibodies against CDK8 (residues 397–414), CDK19 (residues 377–399), and antibodies against full-length MED4, MED7, MED9, and MED17, were raised in rabbits (Cocalico Biologicals, Inc.).

EM Analysis of Mediator-GST-CTD and Mediator-RNAPII Interaction

GST-CTD- 6xHis was expressed in *E. coli* and purified by using Ni-NTA agarose (Qiagen) following standard procedures. To determine the location of GST-CTD binding on Mediator, purified Mediator was added to GST-CTD bound to glutathione Sepharose beads and incubated for 4h at 4°C. Complexes were eluted from the resin, negatively stained, and examined by EM as described above. The 6xHis-tagged CTD was obtained after removal of GST from GST-CTD-6xHis. Localization of a 6xHis-tagged CTD on Mediator was carried out by incubating equimolar amounts of Mediator and 6xHis-tagged CTD with a 3-fold molar excess of anti-His antibodies (Genscript, A00186) for 2h at 4°C. To RNAPII binding position on Mediator was determined by mixing Mediator with a 2-fold molar excess of RNAPII for 4h at 4°C. The resulting complexes were negatively stained and examined by EM as described above.

Supplementary Material

Refer to Web version on PubMed Central for supplementary material.

Acknowledgments

This work was supported by US National Institutes of Health grants R01 67167 (F.J.A.) and RO1 GM41628 (R.C.C. and J.W.C) and by a grant to the Stowers Institute from the Helen Nelson Medical Research Fund at the Greater Kansas City Community Foundation. Information about the human Mediator–CDK8 interaction came from re-analysis of samples originally provided by Sohail Malik and Robert Roeder (The Rockefeller University, New York, New York, USA). We thank Yuichiro Takagi (Indiana University School of Medicine, Indianapolis, Indiana, USA) for providing purified recombinant Gcn4 and Head module, and for helpful comments about the manuscript. We thank Richard A. Young (Whitehead Institute for Biomedical Research, Cambridge, Massachusetts, USA) for providing yeast strains Z695 and Z735 bearing the Srb8-1 and Srb10-1 mutations. We also acknowledge the National Resource for Automated Macromolecular Microscopy (NRAMM).

References

1. Takagi Y, Kornberg RD. Mediator as a general transcription factor. J Biol Chem. 2006; 281:80–89. [PubMed: 16263706]
2. Baek HJ, Malik S, Qin J, Roeder RG. Requirement of TRAP/mediator for both activator-independent and activator-dependent transcription in conjunction with TFIID-associated TAF(II)s. Mol Cell Biol. 2002; 22:2842–2852. [PubMed: 11909976]
3. Flanagan PM, Kelleher RJ 3rd, Sayre MH, Tschochner H, Kornberg RD. A mediator required for activation of RNA polymerase II transcription in vitro. Nature. 1991; 350:436–438. [PubMed: 2011193]
4. Flanagan PM, et al. Resolution of factors required for the initiation of transcription by yeast RNA polymerase II. J Biol Chem. 1990; 265:11105–11107. [PubMed: 2193032]
5. Cai G, Imasaki T, Takagi Y, Asturias FJ. Mediator structural conservation and implications for the regulation mechanism. Structure. 2009; 17:559–567. [PubMed: 19368889]

6. Hengartner CJ, et al. Temporal regulation of RNA polymerase II by Srb10 and Kin28 cyclin-dependent kinases. Mol Cell. 1998; 2:43–53. [PubMed: 9702190]
7. Liao SM, et al. A kinase-cyclin pair in the RNA polymerase II holoenzyme. Nature. 1995; 374:193–196. [PubMed: 7877695]
8. Nonet ML, Young RA. Intragenic and extragenic suppressors of mutations in the heptapeptide repeat domain of Saccharomyces cerevisiae RNA polymerase II. Genetics. 1989; 123:715–724. [PubMed: 2693207]
9. Donner AJ, Ebmeier CC, Taatjes DJ, Espinosa JM. CDK8 is a positive regulator of transcriptional elongation within the serum response network. Nat Struct Mol Biol. 2010; 17:194–201. [PubMed: 20098423]
10. Knuesel MT, Meyer KD, Donner AJ, Espinosa JM, Taatjes DJ. The human CDK8 subcomplex is a histone kinase that requires Med12 for activity and can function independently of mediator. Mol Cell Biol. 2009; 29:650–661. [PubMed: 19047373]
11. Donner AJ, Szostek S, Hoover JM, Espinosa JM. CDK8 is a stimulus-specific positive coregulator of p53 target genes. Mol Cell. 2007; 27:121–133. [PubMed: 17612495]
12. Borggrefe T, Davis R, Erdjument-Bromage H, Tempst P, Kornberg RD. A complex of the Srb8, -9, -10, and -11 transcriptional regulatory proteins from yeast. J Biol Chem. 2002; 277:44202–44207. [PubMed: 12200444]
13. Hengartner CJ, et al. Association of an activator with an RNA polymerase II holoenzyme. Genes Dev. 1995; 9:897–910. [PubMed: 7774808]
14. Myers LC, et al. The Med proteins of yeast and their function through the RNA polymerase II carboxy-terminal domain. Genes Dev. 1998; 12:45–54. [PubMed: 9420330]
15. Spahr H, et al. Mediator influences Schizosaccharomyces pombe RNA polymerase II-dependent transcription in vitro. J Biol Chem. 2003; 278:51301–51306. [PubMed: 14534314]
16. Taatjes DJ, Naar AM, Andel F 3rd, Nogales E, Tjian R. Structure, function and activator-induced conformations of the CRSP coactivator. Science. 2002; 295:1058–1062. [PubMed: 11834832]
17. Holstege FC, et al. Dissecting the regulatory circuitry of a eukaryotic genome. Cell. 1998; 95:717–728. [PubMed: 9845373]
18. Knuesel MT, Meyer KD, Bernecky C, Taatjes DJ. The human CDK8 subcomplex is a molecular switch that controls Mediator coactivator function. Genes Dev. 2009; 23:439–451. [PubMed: 19240132]
19. Elmlund H, et al. The cyclin-dependent kinase 8 module sterically blocks Mediator interactions with RNA polymerase II. Proc Natl Acad Sci U S A. 2006; 103:15788–15793. [PubMed: 17043218]
20. Bernecky C, Grob P, Ebmeier CC, Nogales E, Taatjes DJ. Molecular architecture of the human Mediator-RNA polymerase II-TFIIF assembly. PLoS Biol. 2011; 9:e1000603. [PubMed: 21468301]
21. Puig O, et al. The tandem affinity purification (TAP) method: a general procedure of protein complex purification. Methods. 2001; 24:218–229. [PubMed: 11403571]
22. Radermacher M, Wagenknecht T, Verschoor A, Frank J. Three-dimensional reconstruction from a single-exposure random conical tilt series applied to the 50S ribosomal subunit of *Escherichia coli*. J Microsc. 1987; 146:113–136. [PubMed: 3302267]
23. Schneider EV, et al. The structure of CDK8/CycC implicates specificity in the CDK/cyclin family and reveals interaction with a deep pocket binder. J Mol Biol. 2011; 412:251–266. [PubMed: 21806996]
24. Kang JS, et al. The structural and functional organization of the yeast mediator complex. J Biol Chem. 2001; 276:42003–42010. [PubMed: 11555651]
25. Dotson MR, et al. Structural organization of yeast and mammalian mediator complexes. Proc Natl Acad Sci. 2000; 97:14307–14310. [PubMed: 11114191]
26. Imasaki T, et al. Architecture of the Mediator head module. Nature. 2011; 475:240–243. [PubMed: 21725323]
27. Robinson PJ, Bushnell DA, Trnka MJ, Burlingame AL, Kornberg RD. Structure of the Mediator Head module bound to the carboxy-terminal domain of RNA polymerase II. Proc Natl Acad Sci U S A. 2012; 109:17931–17935. [PubMed: 23071300]

28. Lariviere L, et al. Structure of the Mediator head module. Nature. 2012
29. Naar AM, Taatjes DJ, Zhai W, Nogales E, Tjian R. Human CRSP interacts with RNA polymerase II CTD and adopts a specific CTD-bound conformation. Genes Dev. 2002; 16:1339–1344. [PubMed: 12050112]
30. Asturias FJ, Jiang YW, Myers LC, Gustafsson CM, Kornberg RD. Conserved structures of mediator and RNA polymerase II holoenzyme. Science. 1999; 283:985–987. [PubMed: 9974391]
31. Davis JA, Takagi Y, Kornberg RD, Asturias FA. Structure of the yeast RNA polymerase II holoenzyme: Mediator conformation and polymerase interaction. Mol Cell. 2002; 10:409–415. [PubMed: 12191485]
32. Yang Z, Fang J, Chittuluru J, Asturias FJ, Penczek PA. Iterative Stable Alignment and Clustering of 2D Transmission Electron Microscope Images. Structure. 2012; 20:237–247. [PubMed: 22325773]
33. Cai G, et al. Interaction of the Mediator Head Module with RNA Polymerase II. Structure. 2012; 20:899–910. [PubMed: 22579255]
34. Svejstrup JQ, et al. Evidence for a mediator cycle at the initiation of transcription. Proc Natl Acad Sci. 1997; 94:6075–6078. [PubMed: 9177171]
35. Penczek PA, Kimmel M, Spahn CM. Identifying conformational states of macromolecules by eigen-analysis of resampled cryo-EM images. Structure. 2011; 19:1582–1590. [PubMed: 22078558]
36. Brignole EJ, Smith S, Asturias FJ. Conformational flexibility of metazoan fatty acid synthase enables catalysis. Nat Struct Mol Biol. 2009; 16:190–197. [PubMed: 19151726]
37. Cai G, et al. Mediator head module structure and functional interactions. Nat Struct Mol Biol. 2010; 17:273–279. [PubMed: 20154708]
38. Frank J, et al. SPIDER and WEB: Processing and visualization of images in 3D electron microscopy and related fields. J Struct Biol. 1996; 116:190–199. [PubMed: 8742743]
39. Hohn M, et al. SPARX, a new environment for Cryo-EM image processing. J Struct Biol. 2007; 157:47–55. [PubMed: 16931051]
40. Voss NR, Yoshioka CK, Radermacher M, Potter CS, Carragher B. DoG Picker and TiltPicker: software tools to facilitate particle selection in single particle electron microscopy. J Struct Biol. 2009; 166:205–213. [PubMed: 19374019]
41. Pettersen EF, et al. UCSF Chimera--a visualization system for exploratory research and analysis. J Comput Chem. 2004; 25:1605–1612. [PubMed: 15264254]
42. Sato S, et al. Identification of mammalian Mediator subunits with similarities to yeast Mediator subunits Srb5, Srb6, Med11, and Rox3. J Biol Chem. 2003; 278:15123–15127. [PubMed: 12584197]
43. Morita S, Kojima T, Kitamura T. Plat-E: an efficient and stable system for transient packaging of retroviruses. Gene Ther. 2000; 7:1063–1066. [PubMed: 10871756]

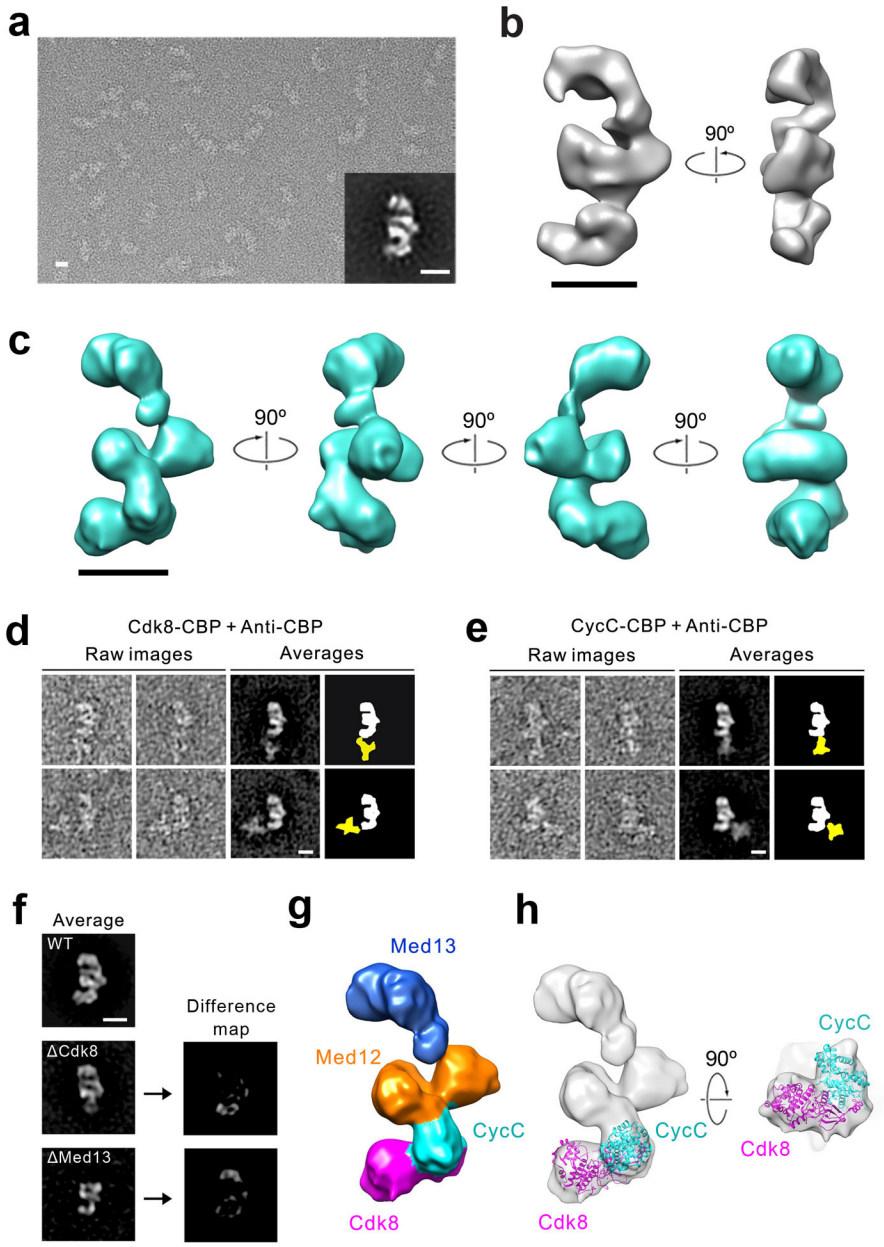

Figure 1. EM analysis and subunit organization of yeast CKM

(**a**) An EM image showing single CKM particles preserved in uranyl acetate. The inset shows a corresponding 2D class average. (**b**) Different views of a 3D map of the CKM calculated from images of stained CKM particles. (**c**) Different views of a cryo-EM map of the CKM. (**d**) Antibody labeling of a CBP tag left at the C-terminus of Cdk8 after TAP-purification. Raw particle images (left) and class averages (right, with antibody density colored in yellow) localize Cdk8 to the distal lower end of the CKM structure. (**e**) Antibody labeling of a CBP tag left at the CycC C-terminus after TAP-purification. (**f**) Comparison of class averages obtained from images of wild-type, ΔMed13, and ΔCdk8 CKMs. (**g**) Subunit organization of the yeast CKM derived from subunit labeling and difference mapping results. Med12 was not localized directly, but its position could be inferred after localization

of the 3 other CKM subunits. (**h**) Docking of an X-ray model of the human CycC-Cdk8 complex into our cryo-EM map of the yeast CKM. Two different views illustrate the close correspondence between the structure of the human complex and the corresponding portion of the yeast cryo-EM map.

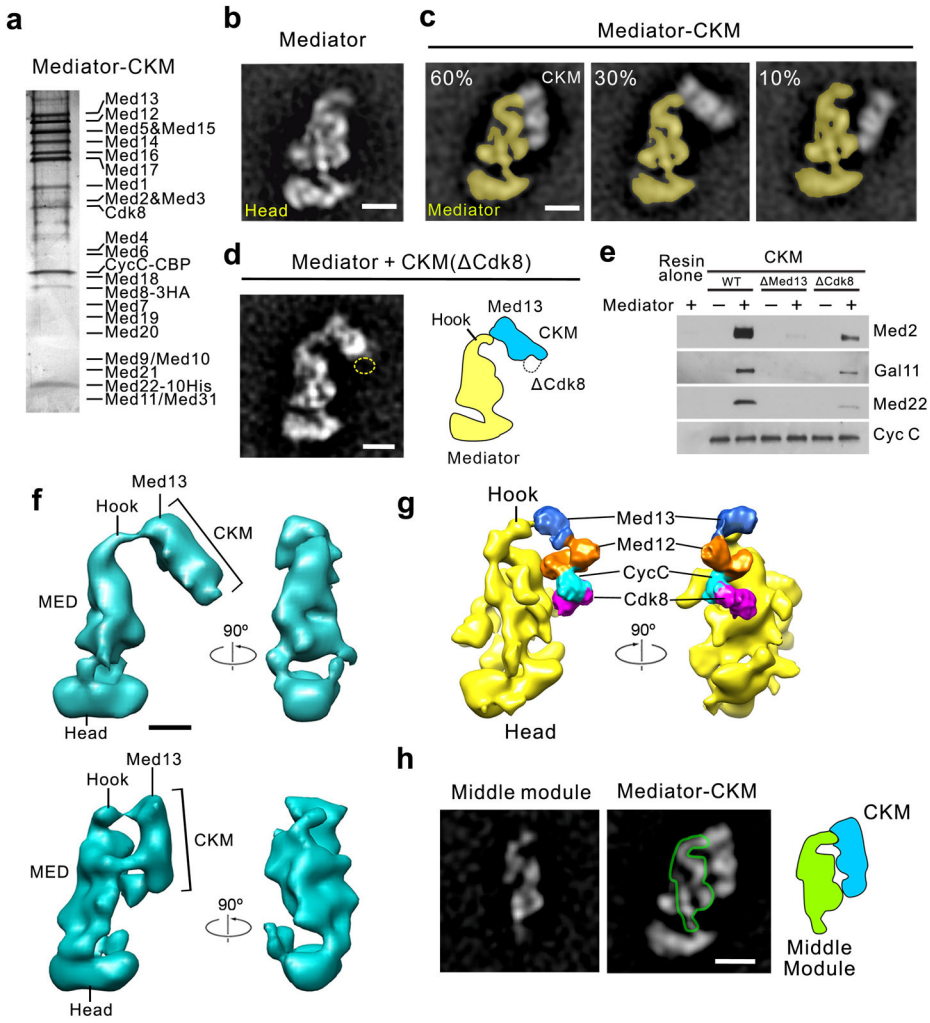

Figure 2. Mediator-CKM interaction in yeast

(**a**) Silver-stained SDS-PAGE analysis of a Mediator-CKM complex purified through a CBP tag on the CycC CKM subunit. (**b**) A 2D class average of Mediator alone. (**c**) Different arrangements of Mediator-bound CKM were identified through reference–free alignment and classification of EM images. The CKM can be tightly associated through a large interface (left), or either end of the CKM structure can establish a single contact with Mediator (middle and right). Mediator density is colored yellow to distinguish it from the CKM. (**d**) Class average calculated from images of particles obtained after incubation of Mediator with ΔCdk8 CKM. The image shows that Med13 contacts the “hook” at the top of the Mediator structure, and that contacts with other portions of Mediator are absent after deletion of Cdk8 (which would have been located around the area indicated by the dashed circle). (**e**) Binding between Mediator and wild-type, ΔMed13, or ΔCdk8 CKM. Wild-type CKM shows the strongest binding, likely due to a large Mediator-CKM interface. The Mediator-CKM interaction is weakened by deletion of Cdk8, and all but eliminated by deletion of Med13, suggesting that the Med13-Tail contact is stronger than the Cdk8-Middle contact. (**f**) 3D maps of two conformations of the yeast Mediator-CKM complex showing a single contact between Mediator and the Med13 CKM subunit (top), and an extended

Mediator-CKM interface (bottom). (**g**) A 3D model of the yeast Mediator–CKM interaction based on cryo-EM maps of Mediator and the CKM, and on the second 3D map of the yeast Mediator–CKM complex shown in (f). Mediator is in yellow. CKM subunits are color-coded as indicated. (**h**) A 2D class average of the yeast Mediator Middle module (left) compared to a 2D class average of the yeast Mediator–CKM complex (right). As indicated by the green outline, the Middle module appears to comprise all domains contacted by the yeast CKM. All scale bars represent 10 nm.

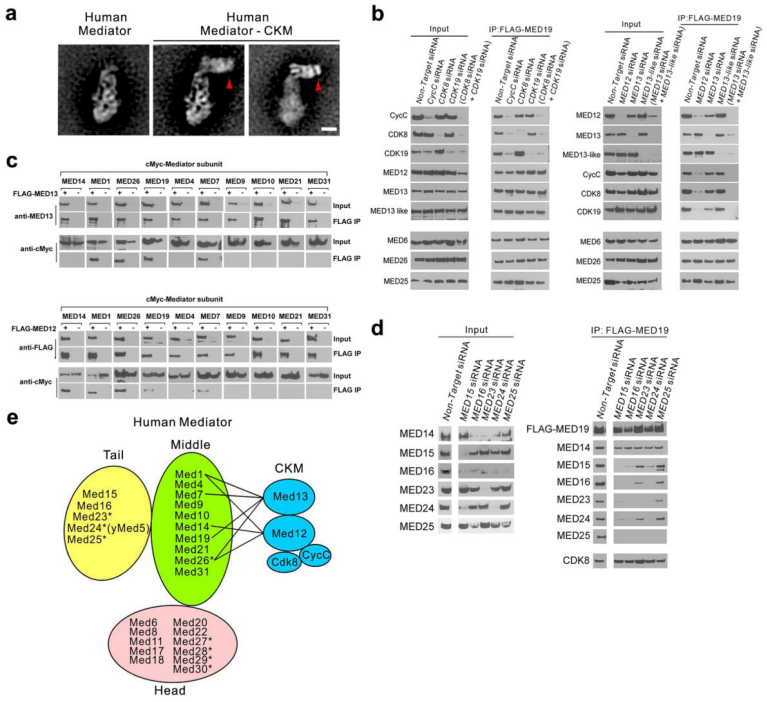

Figure 3. Human Mediator–CKM interaction

(**a**) 2D EM analysis of the human Mediator-CKM complex showing class averages of human Mediator alone (left), the human Mediator-CKM complex (middle), and the human Mediator-CKM complex with alignment focused only on the CKM (right). (**b**) Immunoblot analysis of the human Mediator–CKM interaction following siRNA-mediated knockdown of various CKM subunits. CDK19 is an isoform of CDK8 considered a component of the human Mediator. (**c**) Immunoblot analysis of human Middle module–CKM subunit interactions following exogenous expression of FLAG-tagged MED12 or MED13. (**d**) Immunoblot analysis of the human Mediator–CKM interaction following siRNA-mediated knockdown of Tail module subunits. (**e**) Summary of human Mediator–CKM subunit interaction results. The names of human Mediator subunits not present in yeast Mediator are marked by asterisks.

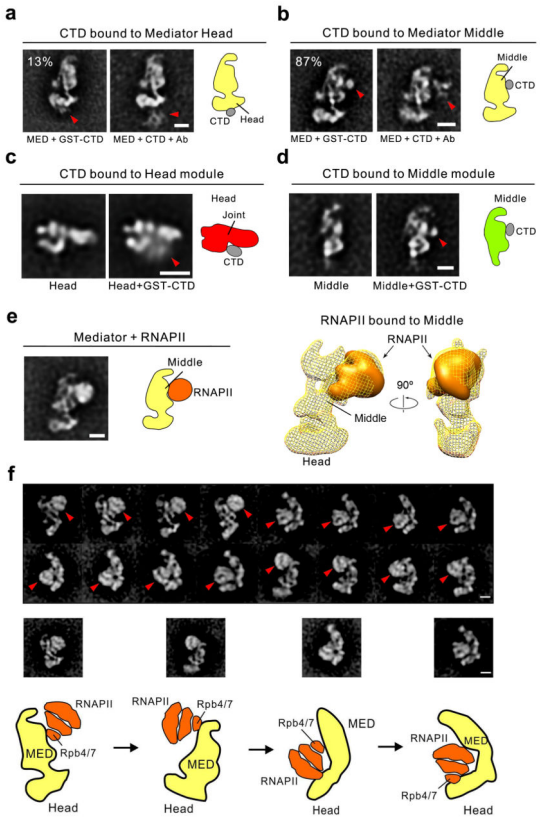

Figure 4. Mediator–CTD and Mediator–RNAPII interaction in yeast

(**a**) EM analysis of the Mediator-CTD interaction indicates that ~13% of particles show GST-CTD density next to the Head Mediator module (left, red arrow). Labeling of Mediator-bound 6xHis-CTD with anti-His antibodies also localizes the CTD to that same area adjacent to the Head (middle, red arrow). A diagram summarizing this result is shown in the right panel. (**b**) EM analysis of the Mediator-CTD interaction indicates that ~87% of particles show GST-CTD density next to the Middle Mediator module (left, red arrow). Labeling of Mediator-bound 6xHis-CTD with anti-His antibodies also localizes the CTD to that same area adjacent to the Middle module (middle, red arrow). A diagram summarizing this result is shown in the right panel. (**c**) 2D class averages of a recombinant Head module alone (left) and after incubation with a GST-CTD (middle), and a diagram summarizing this result (right). (**d**) 2D class averages of purified Middle module alone (left) and after incubation with a GST-CTD (middle), and a diagram summarizing this result (right). (**e**) A class average (left) and a 3D EM map (right, map in yellow mesh with a fitted low-pass filtered RNAPII model in orange) showing the structure of the predominant complex formed after incubation of Mediator with RNAPII, with RNAPII located next to the CTD-binding site on the Middle module. (**f**) Class averages obtained after clustering of holoenzyme particles purified from yeast show RNAPII interacting with the Middle and Head modules, and at various intermediate positions. Diagrams representing the main complex configurations are shown below the class averages. All scale bars represent 10 nm.

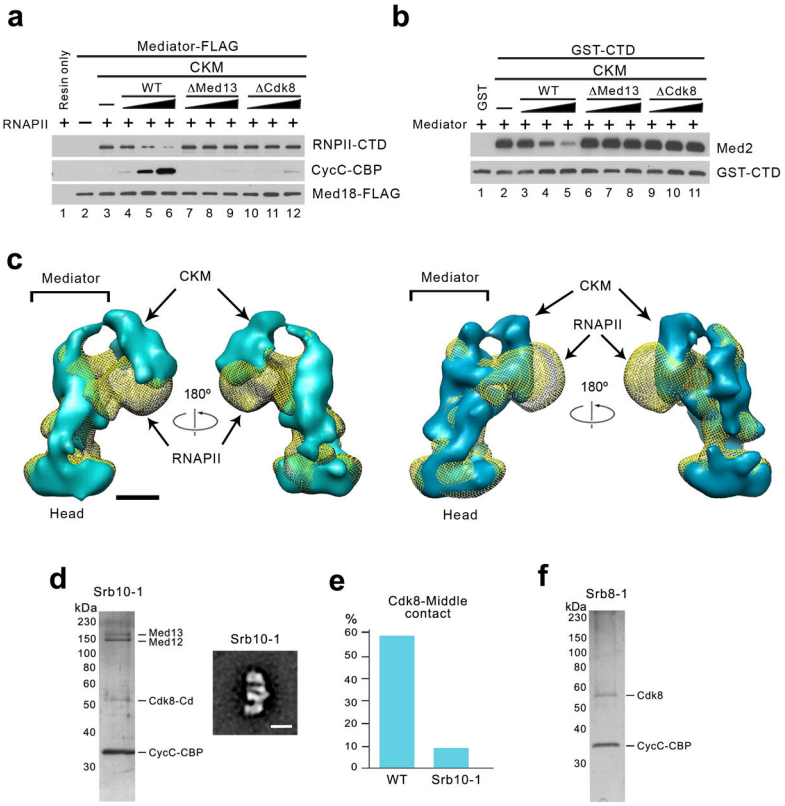

Figure 5. Interplay between CKM and RNAPII interaction with Mediator

(**a**) Interaction of Mediator with RNAPII in the presence of wild-type, ΔMed13, or ΔCdk8 CKM. Under this assay conditions, wild-type CKM blocks interaction of RNAPII with Mediator, but ΔMed13 CKM or ΔCdk8 CKM have no effect. (**b**) Interaction of GST-CTD with Mediator in the presence of wild-type, ΔMed13 or ΔCdk8 CKM. The effect of the different CKMs on CTD interaction with Mediator mirrors their effect on RNAPII interaction. (**c**) Comparison between 3D EM maps of Mediator–RNAPII and Mediator–CKM complexes highlights the overlap between RNAPII and CKM densities that results from binding of both to the same portion of the Mediator structure. (**d**) Silver-stained SDS-PAGE analysis of purified Srb10-1 CKM comprising Med13, Med12, CycC, and a C-terminal truncated Cdk8 (Cdk8-Cd) kinase (left). A class average calculated from images of Srb10-1 CKM particles shows that the CKM complex appears intact (the C-terminal deletion in Cdk8 is too small to be apparent at the resolution of the class average). (**e**) Effect of the Srb10-1 Cdk8 C-terminal truncation on Mediator-CKM interaction. Nearly 60% of Mediator-CKM particles formed with wild-type CKM show the Cdk8-Middle module contact. In contrast, only ~10% of Mediator-CKM particles formed with Srb10-1 CKM show a contact with the Middle module. (**f**) Silver-stained SDS-PAGE analysis of purified Srb8-1 CKM shows that it only contains CycC and the Cdk8 kinase. All scale bars represent 10 nm.

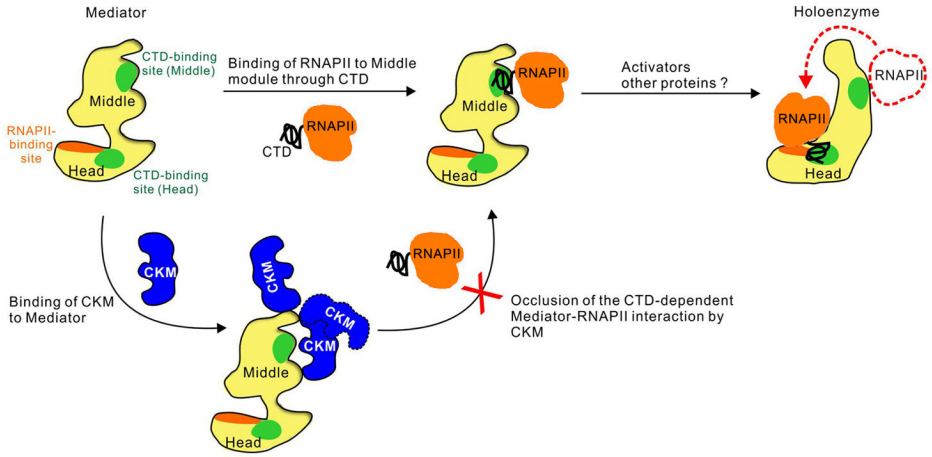

Figure 6.

A model for CKM-dependent repression through obstruction of CTD-dependent Mediator–RNAPII interaction. An initial CTD-dependent contact of RNAPII with the Middle Mediator module is obstructed by Mediator–CKM interaction. Details of the steps that would result in movement of RNAPII from the Middle to the Head modules and formation of the holoenzyme remain to be investigated. Mediator is shown in yellow, and the CKM and RNAPII in blue and orange, respectively.